



High-resolution ellipsometric study of an n-alkane film, dotriacontane, adsorbed on a SiO₂ surface

Volkman, U.G.; Pino, M.; Altamirano, L.A.; Taub, H.; Hansen, Flemming Yssing

Published in:
Journal of Chemical Physics

Link to article, DOI:
[10.1063/1.1429645](https://doi.org/10.1063/1.1429645)

Publication date:
2002

Document Version
Publisher's PDF, also known as Version of record

[Link back to DTU Orbit](#)

Citation (APA):
Volkman, U. G., Pino, M., Altamirano, L. A., Taub, H., & Hansen, F. Y. (2002). High-resolution ellipsometric study of an n-alkane film, dotriacontane, adsorbed on a SiO₂ surface. *Journal of Chemical Physics*, 116(5), 2107-2115. <https://doi.org/10.1063/1.1429645>

General rights

Copyright and moral rights for the publications made accessible in the public portal are retained by the authors and/or other copyright owners and it is a condition of accessing publications that users recognise and abide by the legal requirements associated with these rights.

- Users may download and print one copy of any publication from the public portal for the purpose of private study or research.
- You may not further distribute the material or use it for any profit-making activity or commercial gain
- You may freely distribute the URL identifying the publication in the public portal

If you believe that this document breaches copyright please contact us providing details, and we will remove access to the work immediately and investigate your claim.

High-resolution ellipsometric study of an *n*-alkane film, dotriacontane, adsorbed on a SiO₂ surface

U. G. Volkman, M. Pino, and L. A. Altamirano^{a)}

Facultad de Física, Pontificia Universidad Católica de Chile, Santiago, Chile

H. Taub^{b)}

Department of Physics and Astronomy and University of Missouri Research Reactor, University of Missouri-Columbia, Columbia, Missouri 65211

F. Y. Hansen

Department of Chemistry, Technical University of Denmark, IK 207 DTU, DK-2800 Lyngby, Denmark

(Received 1 August 2001; accepted 31 October 2001)

Using high-resolution ellipsometry and stray light intensity measurements, we have investigated during successive heating-cooling cycles the optical thickness and surface roughness of thin dotriacontane ($n\text{-C}_{32}\text{H}_{66}$) films adsorbed from a heptane ($n\text{-C}_7\text{H}_{16}$) solution onto SiO₂-coated Si(100) single-crystal substrates. Our results suggest a model of a solid dotriacontane film that has a phase closest to the SiO₂ surface in which the long-axis of the molecules is oriented *parallel* to the interface. Above this “parallel film” phase, a solid monolayer adsorbs in which the molecules are oriented *perpendicular* to the interface. At still higher coverages and at temperatures below the bulk melting point at $T_b = 341$ K, solid bulk particles coexist on top of the “perpendicular film.” For higher temperatures in the range $T_b < T < T_s$ where $T_s = 345$ K is the wetting temperature of the bulk phase, the coexisting bulk particles melt into droplets; and for $T > T_s$, a uniformly thick fluid film wets to the parallel film phase. This structure of the alkane/SiO₂ interfacial region differs qualitatively from that which occurs in the surface freezing effect at the bulk alkane fluid/vapor interface. In that case, there is again a perpendicular film phase adjacent to the air interface but no parallel film phase intervenes between it and the bulk alkane fluid. Similarities and differences between our model of the alkane/SiO₂ interface and one proposed recently will be discussed. Our ellipsometric measurements also show evidence of a crystalline-to-plastic transition in the perpendicular film phase similar to that occurring in the solid bulk particles present at higher coverages. In addition, we have performed high-resolution ellipsometry and stray-light measurements on dotriacontane films deposited from solution onto highly oriented pyrolytic graphite substrates. After film deposition, these substrates proved to be less stable in air than SiO₂.

© 2002 American Institute of Physics. [DOI: 10.1063/1.1429645]

I. INTRODUCTION

Very high-resolution ellipsometry (VHRE) has proved to be an effective method of studying the wetting behavior, growth mode, and multilayer phase diagrams of physisorbed films.^{1,2} The VHRE technique is extremely sensitive to the average film thickness. It is capable of detecting a change in the number of adsorbed molecules on the order of one per cent of a monolayer. This sensitivity corresponds to a change in film thickness of ~ 0.05 Å averaged over the illuminated sample area.²

Heretofore, VHRE has been applied exclusively to films of rare gases and relatively small molecules deposited from the vapor phase onto highly oriented pyrolytic graphite (HOPG) substrates held below room temperature in ultra-high vacuum. One of our motivations in the present work is to extend the VHRE technique to films of larger molecules deposited from solution onto substrates that are

not only of fundamental interest but are also technologically important. For this purpose, we have been investigating films of several intermediate-length normal alkanes [$n\text{-CH}_3(\text{CH}_2)_{n-2}\text{CH}_3$; $20 < n < 40$] adsorbed from a solution with heptane ($n=7$) onto Si(100) substrates. Alkanes of this length are of technological interest as the principal constituents of commercial lubricants. They are also of fundamental interest as prototypes of more complex polymers.³ The Si(100) substrates are commercially available wafers widely used in the semiconductor industry. They provide large, high-quality single-crystal surfaces with few defects. The wafers can be polished to microscopic smoothness and cut into samples that are mechanically stable when immersed in the alkane solution.

In this paper, we shall describe VHRE experiments and stray light intensity (SLI) measurements conducted in air on dotriacontane films ($n=32$ or C32) at room temperature and above. Since the Si(100) substrates readily oxidize in air, the adsorbing surface of our wafers is actually provided by a silicon-oxide (SiO₂) coating less than ~ 25 Å thick as determined by x-ray specular reflectivity measurements.

^{a)}Present address: Dicontek, Casilla 306, Santiago 22, Chile.

^{b)}Electronic mail: taubh@missouri.edu

Due to the large number of experimental studies of intermediate-length *n*-alkanes adsorbed on graphite substrates (for a brief review, see Ref. 3), we were also motivated to conduct similar high-resolution ellipsometric and stray light intensity measurements on HOPG substrates. As will be discussed below, these substrates proved to be much less stable in air after dipping into the alkane solution due to their microcrystallinity and the effects of thermal expansion during heating cycles. In fact, we were only able to interpret the ellipsometric and stray light intensity measurements on the HOPG samples after analyzing results from the Si(100)/SiO₂ substrates.

The wetting behavior of alkanes on SiO₂ surfaces has been studied previously by optical microscopy, x-ray reflectivity, and conventional ellipsometry.^{4–7} For alkanes containing 16 to 50 carbon atoms and film thicknesses of several hundred angstroms, Merkl *et al.*⁴ have presented a model comprising three different wetting topologies on the SiO₂ surface: (1) for temperatures $T < T_b$ where T_b is the bulk alkane melting point, there is incomplete wetting. A bulk alkane phase in the form of small crystallites (frozen droplets) resides atop a solid monolayer adjacent to the SiO₂ surface in which the molecules are oriented normal to the interface. The bulk particles can be annealed into mesas of uniform height; (2) for $T_b < T < T_s$ where T_s is the wetting temperature, the bulk crystallites melt into liquid droplets; and (3) for $T > T_s$, there is complete wetting of a uniformly thick liquid alkane film to the SiO₂ surface. Thus, in the model of Merkl *et al.*, the wetting temperature $T_s \approx T_b + 3$ K coincides with the melting or disordering temperature of their proposed monolayer phase. The persistence of the solid monolayer phase in the temperature range $T_b < T < T_s$ resembles the surface freezing phenomenon observed in bulk alkanes at the liquid–vapor interface.⁸ This led Merkl *et al.* to conclude that a common surface freezing mechanism was operative at both interfaces.

The C32 films adsorbed on SiO₂-coated Si(100) substrates which we investigate here have an average thickness up to ~ 110 Å. The thinness of our C32 films and the high resolution of our ellipsometer allow us to resolve features that were not reported by Merkl *et al.*⁴ For films having an average thickness ≥ 50 Å, the temperature dependence of the polarization angle of the reflected light is consistent with the three wetting topologies that they propose. However, our results on films having an average thickness less than the all-*trans* length of the molecule (~ 44 Å for C32) conflict with their model. Our ellipsometer measurements indicate that it is possible to adsorb uniform solid C32 films of thickness down to ≤ 4.5 Å, i.e., a thickness on the order of the molecular width.

II. EXPERIMENT

The ellipsometer used in these experiments has been described previously.⁹ Briefly, it employs the PCSA configuration (polarizer, Soleil-Babinet compensator, sample, analyzer). After passing through a polarizer and compensator, light from a He–Ne laser (wavelength $\lambda = 6328$ Å) is incident on the sample at an angle of 60° to the surface normal and illuminates an area of ~ 1 mm². Reflected light from the

sample passes through the analyzer and enters the photodetector. For planar films thin compared to λ , the changes in polarizer angle dP and analyzer angle $d\Psi$ are proportional to the film thickness averaged over the illuminated sample area. If the films are rough, dP cannot be related to an average film thickness because it depends on the length scale of the roughness. Since dP is about an order of magnitude larger than $d\Psi$, the average optical thickness of the adsorbed film is measured by dP with the analyzer angle held fixed. This is accomplished using an electronic feedback loop with a Faraday coil placed between the polarizer and compensator.

We have also measured the diffuse light that is scattered isotropically from the sample due to it having surface roughness on a length scale comparable to the wavelength of the incident laser light. This stray light is observed through a telescope focused on the sample area illuminated by the ellipsometer's laser, and its intensity is measured on a photomultiplier tube. The telescope is aligned at $\sim 35^\circ$ to the sample's surface normal.

In order to interpret the ellipsometric measurements, we used a continuum or Drude model based on Fresnel's equation that relates the ellipsometric angles dP and $d\Psi$ to the index of refraction n and the thickness t of a planar adsorbed film.^{10,11} This method of analysis should be used with some caution. First, our SLI measurements indicate that the adsorbed C32 film does not always have a planar topology. For samples with a coverage high enough to nucleate bulk particles, values of t quoted will be for fluid films at a temperature of $T_s + 3$ K where the approximation of a planar topology should be valid. Below this temperature, our measurements show that there is negligible alkane desorption. Therefore, for samples with a coverage less than that required for bulk nucleation (e.g., sample Si#3 in Fig. 3), we can assume that the average film thickness at the beginning of a heating cycle is the same as at a temperature of $T_s + 3$ K. At even lower coverages where there are insufficient molecules to form a complete planar film, i.e., the adsorbed molecules form islands, the film thickness t inferred from the Drude model will represent an average over the illuminated sample area.

A second reason for care in applying the Drude analysis is that n and t may be poorly defined quantities for films of molecular thickness. However, Volkman and Knorr² have previously demonstrated agreement between the t inferred from the Drude theory and that inferred from a microscopic model for a molecular monolayer.^{12,13}

For calculations with a Drude model, we assume the adsorbed C32 to have a refractive index $n = 1.455$ ¹⁴ and the Si(100)/SiO₂ substrate to have $n = 3.875$ with an imaginary part $k = 0.019$ as reported for pure silicon.¹⁵ We have verified that the SiO₂ coating on our substrates has a negligible effect on our determination of the C32 film thicknesses. Values of n and k inferred from the measured polarizer and analyzer angles for the bare Si(100)/SiO₂ substrates did not differ significantly from those of pure silicon.¹⁵

The Si(100) substrates¹⁶ were cut from a wafer 0.4 mm thick and had a square shape 12 mm \times 12 mm. The samples were either rinsed in pure heptane or baked at 600 °C under

vacuum for 3 h. Modeling of x-ray specular reflectivity measurements on these samples indicates that, as prepared, they have a SiO₂ coating of thickness 15–25 Å.¹⁷

To deposit the alkane film, the Si(100)/SiO₂ substrate exposed to air is dipped in a solution of C32 in heptane (*n*-C₇H₁₆) for about five seconds. The alkanes were purchased from Aldrich and had a purity of 97%. When the substrate is removed from the solution, excess liquid is allowed to run off by tilting the sample. For samples prepared in this manner, we find a nearly linear relationship between the average optical thickness of the C32 film measured on the ellipsometer and the concentration of C32 in the solution. As calibration points, a solution of 17.39 mg of C32 in 20 ml of heptane yielded an average C32 film thickness of ~111 Å; and 6.26 mg of C32 in 20 ml of heptane yielded a ~45 Å-thick C32 film. The average film thickness did not increase upon submerging the substrate in the solution for a longer time or by dipping it into the solution repeatedly. Therefore, we conclude that equilibrium was reached during deposition in which the chemical potential of the adsorbed C32 equaled that of the C32 in solution. During the heating–cooling cycles in which dP and the SLI were measured, the samples were exposed to air and their temperature was varied slowly (~2 K/min). Reproducibility of the steps observed in dP and SLI at the temperatures T_s and T_b between different heating cycles of the same sample and between those of different samples indicates that thermal equilibrium was maintained. Only a small amount of hysteresis was observed when these temperatures were traversed in opposite directions.

The highly oriented pyrolytic graphite (HOPG) substrates (ZYA grade from Union Carbide/Advanced Ceramics) had the same size and shape as those of silicon (12 mm×12 mm) but were 1 mm thick. They were cleaned by baking at 600 °C under vacuum for 8 h.

III. RESULTS

A. Bare substrates

In Fig. 1, we compare the temperature dependence of the change in polarization angle dP of two different bare substrates: (a) a Si(100) crystal coated with SiO₂ and (b) HOPG. Both samples were measured in air after heating them in vacuum for 8 h at a temperature of 600 °C. We see that, for the Si(100)/SiO₂ substrate, dP is very stable and nearly temperature independent. In contrast, HOPG shows a systematic decrease in dP upon heating with short-time fluctuations superimposed. It is interesting to note that the initial value of dP is nearly recovered upon cooling back to room temperature, indicating almost the same long-term stability of the ellipsometer as obtained with the Si(100)/SiO₂ substrate. We conclude from the comparison in Fig. 1 that the Si(100)/SiO₂ substrate is much more favorable than HOPG due to its lower background contribution to dP . This is confirmed in results presented below with C32 films adsorbed on HOPG substrates. In addition, we shall see that there are other problems in ellipsometry experiments with HOPG substrates

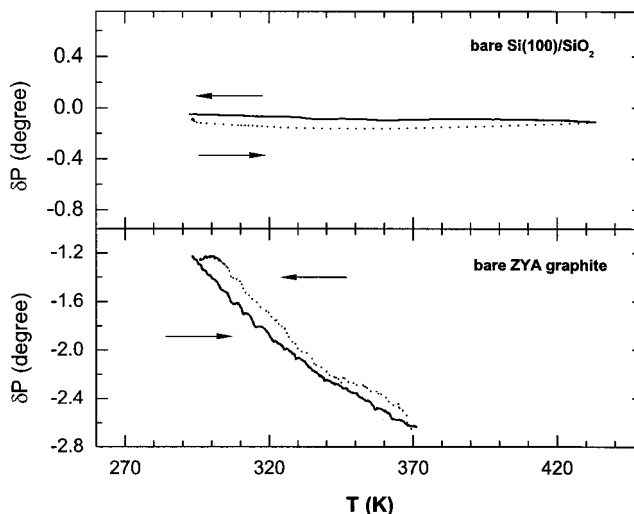


FIG. 1. Change in ellipsometric polarization angle dP as a function of temperature for the bare substrates in air during a heating–cooling cycle. Solid and dotted curves indicate the heating and cooling portions of the cycle, respectively. Upper panel: a Si(100)/SiO₂ wafer. Lower panel: an HOPG sample (ZYA grade from Union Carbide/Advanced Ceramics).

when an alkane film is adsorbed from solution rather than adsorbing the film from the vapor phase as in previous experiments.^{1,2}

B. Thick films

We next consider a series of six heating–cooling cycles in Fig. 2 for one of the thickest samples Si#4 which had an average thickness of ~111 Å as measured above the wetting temperature at $T_s + 3$ K. The dominant feature in the first cycle [Fig. 2(a)] is the complementary behavior of dP and the SLI. There is downward “notch” in the value of dP and an upward notch in the SLI in the temperature range $T_b < T < T_s$ where $T_b = 341$ K is the C32 bulk melting point and $T_s = 345$ K. To facilitate comparison of the temperature dependence of dP and SLI, vertical dashed lines have been drawn in each panel of Fig. 2 at the temperatures T_b and T_s . Above T_s , dP decreases gradually. Upon cooling, both dP and the SLI show a smaller step near T_s than upon heating (there is some hysteresis); and there are no steps in dP and SLI at T_b and below. Thus the first cycle ends with the SLI at a somewhat higher value than it had initially. Another feature to note is a relatively small upward substep in dP upon heating through 336 K.

We expect the SLI to increase when the surface on which the light is incident becomes rough on a length scale comparable to its wavelength. Therefore, the complementary behavior of dP and the SLI in the temperature range $T_b < T < T_s$ for sample Si#4 is in excellent agreement with the presence of bulk liquid droplets of C32 having a characteristic dimension of 1–20 μm inferred by Merkl *et al.*⁴ Also, above T_s , the relatively high value of dP and low SLI that we observe are consistent with the uniformly thick fluid films which they propose. Below T_b , the high value of dP and low SLI observed for this sample after removal from the C32/heptane solution [see Fig. 2(a)] may be due to fewer bulk particles or perhaps a much smaller solid particle size

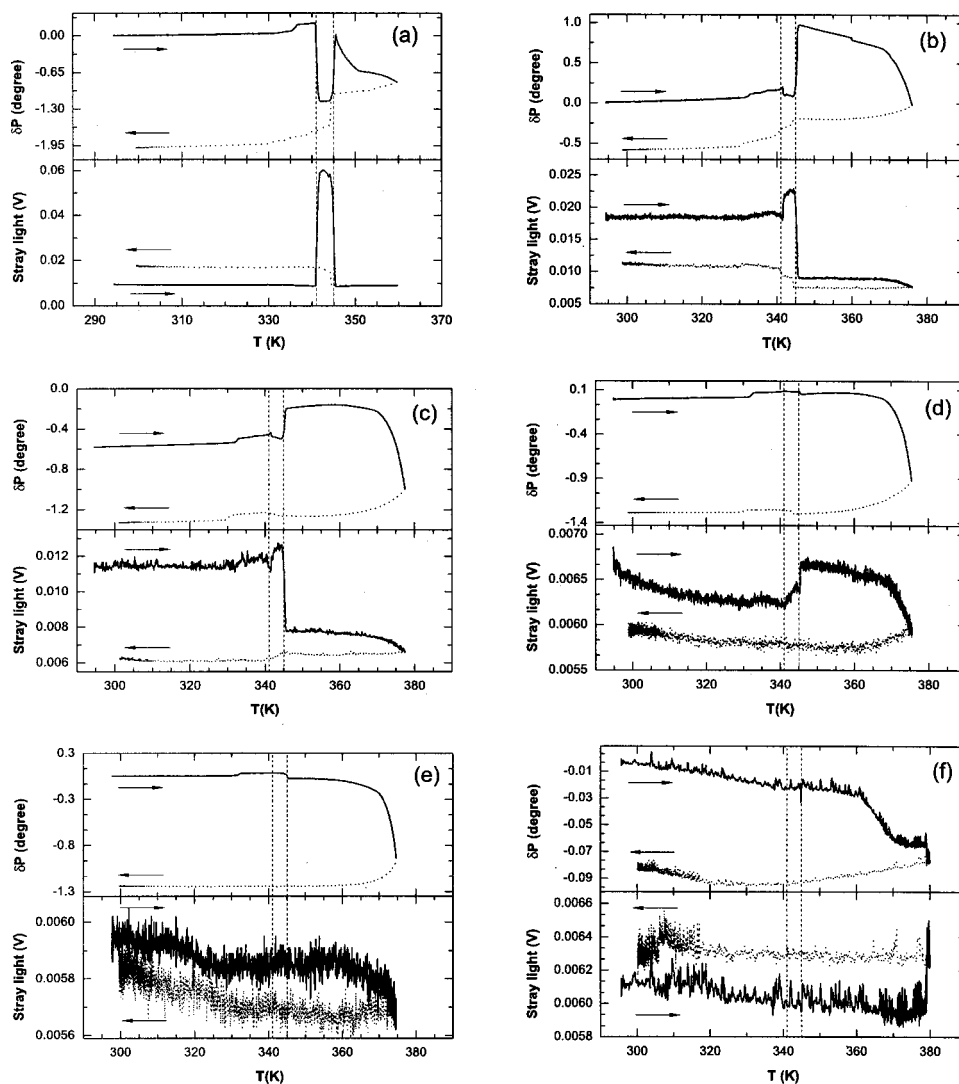


FIG. 2. Change in ellipsometric polarization angle dP (upper panels) and stray light intensity (lower panels) vs temperature for successive heating-cooling cycles of sample Si#4. Solid and dotted curves indicate the heating and cooling portions of the cycle, respectively. The average C32 film thickness at a temperature of $T_s + 3$ K for each cycle is: (a) 111 Å; (b) 93 Å; (c) 71 Å; (d) 50 Å; (e) 24 Å; and (f) 1.4 Å. Note that the final dP angle of each cycle differs from its initial angle in the following cycle. This is caused by the change in dP within a cycle being sufficiently large to require a mechanical readjustment of the ellipsometer.

than that of the liquid droplets. The solid particle size appears to have grown upon resolidification, leading to a higher initial SLI in the next two heating-cooling cycles [Figs. 2(b) and 2(c)].

The complementary temperature dependence of dP and the SLI persists in the next two heating-cooling cycles. In the second cycle [Fig. 2(b)], the average C32 film thickness has decreased to ~ 93 Å at $T_s + 3$ K due to desorption occurring at the highest temperatures in the first cycle. At T_b , both the downward step in dP and the upward step in the SLI are now smaller; however, at T_s , the upward step in dP and the downward step in the SLI are still large. The behavior on cooling is also similar to that in the first cycle, although the downward step in dP at T_s is broadened. Again, there is a small upward step in the SLI coincident with this feature; and, in addition, a second upward substep occurs near T_b . Unlike the first cycle, the SLI ends at a lower level than at which it started, close to its minimum value in the first cycle. This is probably caused by desorption which has reduced the number of bulk particles that can contribute to the SLI. Upon heating, there is still an upward substep in dP below T_b , but now it occurs at a lower temperature of ~ 332 K. This feature

remains in all subsequent cycles except the last one shown in Fig. 2(f).

The average C32 film thickness of sample Si#4 at the beginning of its third heating-cooling cycle [Fig. 2(c)] has decreased to ~ 71 Å at $T_s + 3$ K again due to desorption occurring in the previous cycle at the highest temperatures. Note the increase of the desorption rate at $T \geq 370$ K in Figs. 2(b)–2(e). During the cooling portion of the third cycle, when the average C32 film thickness has decreased to ~ 50 Å, a qualitative change occurs in the temperature dependence of the SLI. Instead of a step upward in the SLI at T_s , there is a broad substep downward. This change signals a qualitatively different behavior of both dP and the SLI in the last three cycles.

In the fourth and fifth heating-cooling cycles [Figs. 2(d) and 2(e), respectively], the dominant feature of the first three cycles has disappeared. That is, there is no longer the complementary behavior of dP and the SLI characterized by a downward “notch” in the value of dP and an upward notch in the SLI in the temperature range $T_b < T < T_s$. The substep upward in dP at ~ 332 K remains upon heating and is followed by a comparably sized downward substep at T_s .

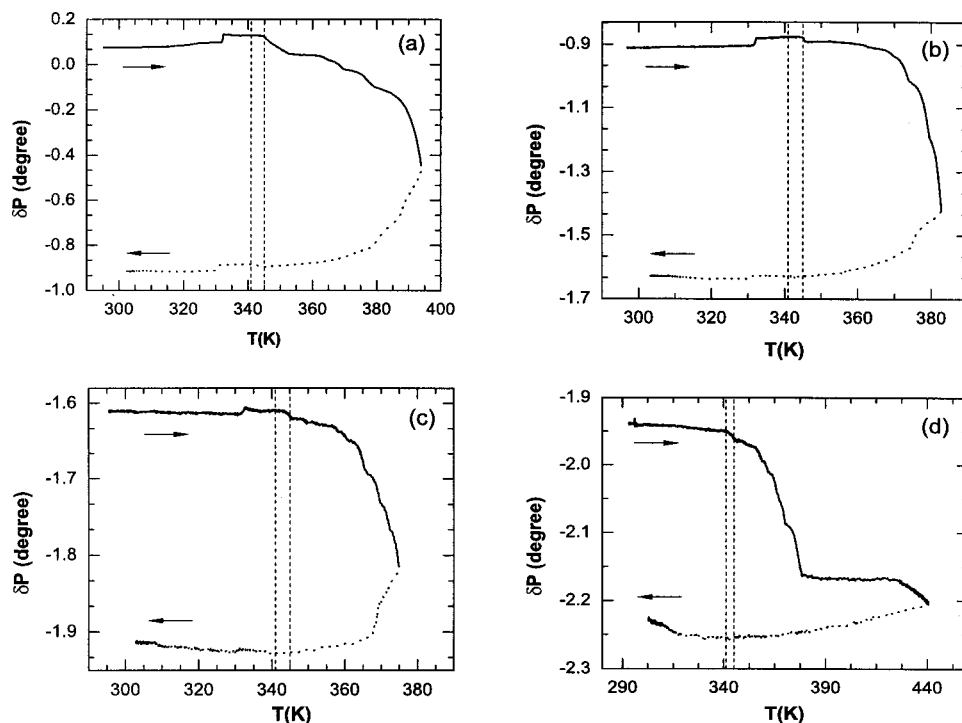


FIG. 3. Change in ellipsometric polarization angle dP versus temperature for successive heating/cooling cycles of sample Si#3. Solid and dotted curves indicate the heating and cooling portions of the cycle, respectively. The initial average C32 film thickness for each cycle is: (a) 45 Å; (b) 26 Å; (c) 12 Å; and (d) 5.6 Å.

In the fourth cycle, this behavior repeats upon cooling, although with some temperature hysteresis. In the cooling half of the fifth cycle and in the sixth cycle [Fig. 2(f)], these two substeps can no longer be seen. The changes in the SLI are much smaller than in the previous cycles and do not seem to correlate with those in dP (except possibly for the upward substep in SLI at T_s upon heating in the fourth cycle [Fig. 2(d)]). We believe that smoother changes in the SLI in the fifth and sixth heating-cooling cycles [Figs. 2(e) and 2(f)] are too small to be significant.

C. Thin films

We next discuss the temperature dependence of dP for one of our thinner samples Si#3 which had an initial average C32 film thickness ~ 45 Å. This sample is thin enough that nucleation of bulk particles and droplets does not occur. Furthermore, since no desorption occurs up to a temperature of $T_s + 3$ K at which the film thickness is calculated from the Drude theory, we shall assume the film has the same average thickness up to this temperature.

In the first heating-cooling cycle shown in Fig. 3(a), we see a behavior very similar to that of sample Si#4 in its fourth cycle [Fig. 2(d)] where it had an initial average C32 film thickness of ~ 50 Å. Little change in dP occurs until a temperature of ~ 332 K at which there is a small upward substep dP to a new constant value followed by a downward substep in dP at $T_s = 345$ K. These two substeps in dP at ~ 332 K and ~ 345 K are also present upon cooling, although displaced slightly downward in temperature. The decrease of dP in the first cycle at temperatures $T > T_s$ results from desorption which reduces the average C32 film thickness by ~ 19 Å. As in the case of sample Si#4, the desorption rate increases above ~ 370 K [see Figs. 3(a)–3(d)].

In the second cycle of Si#3 [Fig. 3(b)], the film has an initial average thickness of ~ 26 Å and shows substeps upon heating similar to those in the first cycle. However, upon cooling, the substep at ~ 345 K is too weak to resolve. By the third cycle [Fig. 3(c)], the initial average film thickness has decreased to ~ 12 Å. The two substeps observed upon heating have decreased in height and are too weak to resolve on cooling. In the fourth cycle [Fig. 3(d)], the initial average film thickness is ~ 6 Å and the two substeps are now absent for both heating and cooling. At temperatures above that of the sharp “corner” in dP near 380 K, the temperature dependence of dP becomes similar to that of the bare substrate in the upper panel of Fig. 1 consistent with complete desorption of the C32 film.

Our results on thin C32 films deposited from solution onto SiO₂ can be summarized as follows. First, it is evident that, for films of comparable thickness, the temperature dependence of dP and the SLI for samples Si#3 and Si#4 are in good agreement. Second, we can progressively thin the C32 film of Si#3 by desorption so that, by the beginning of the fourth heating-cooling cycle [Fig. 3(d)], its average thickness is comparable to a molecular width of ~ 5 Å, and, third, for films of average thickness less than ~ 5 Å, we observe no substeps in dP at temperatures of ~ 332 K and $T_s = 345$ K.

D. Adsorption on HOPG substrates

The reproducible temperature dependence of dP and the SLI for the C32 adsorbed on the Si(100)/SiO₂ substrates allows us to interpret more easily the behavior of these optical properties for C32 adsorbed on an HOPG substrate. In Fig. 4, we show the first two heating-cooling cycles of a C32 film deposited from a C32/heptane solution of about the same concentration as for sample Si#4. The average thickness of the C32 film is ~ 90 Å at a temperature of $T_s + 3$ K [Fig.

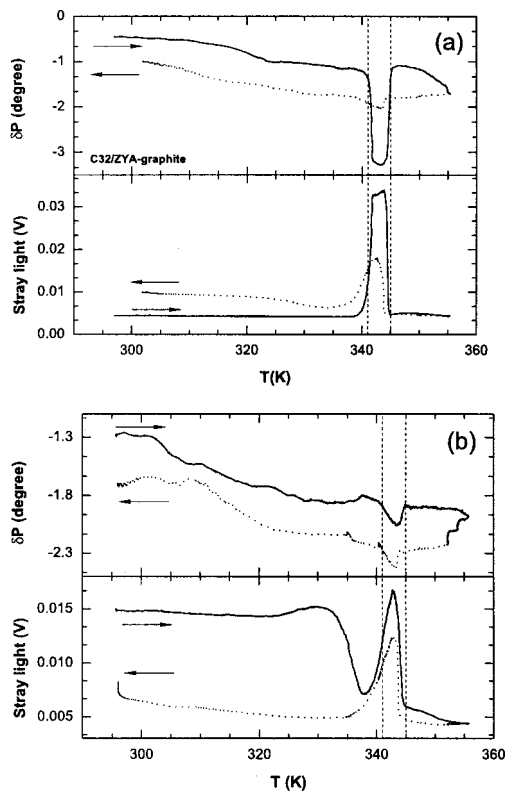


FIG. 4. Change in ellipsometric polarization angle dP (upper panels) and stray light intensity (lower panels) versus temperature for successive heating-cooling cycles of a C32 film adsorbed on an HOPG substrate (ZYA graphite). Solid and dotted curves indicate the heating and cooling portions of the cycle, respectively. The initial average C32 film thickness for each cycle is: (a) 90 Å; (b) 76 Å.

4(a)]. We see that the behavior is qualitatively similar to that of the Si#4 sample in Fig. 2(a). That is, the dominant feature of the dP trace in Fig. 4(a) is the downward notch beginning at the C32 bulk melting point $T_b = 341$ K and ending at $T_s = T_b + 4$ K = 345 K observed both during heating and cooling. As with the Si(100)/SiO₂ substrate, coincident with the downward notch in dP is an upward notch in the SLI.

The main difference with the behavior observed on the Si(100)/SiO₂ substrates is that, as the temperature increases, the downward notch in dP is superimposed on a monotonically decreasing background from the bare HOPG substrate. Also, the sides of the notches in dP and the SLI are not as sharp as on the Si(100)/SiO₂ substrates. These features are greatly enhanced in the cooling portion of the first cycle and in the second cycle [Fig. 4(b)] where the C32 film has an average thickness of ~ 76 Å at $T_s + 3$ K. Here the notches in dP and the SLI have become rounded into a “dip” and “peak,” respectively.

There appears to be more than one effect responsible for the different temperature dependence of dP and the SLI on the Si(100)/SiO₂ and HOPG substrates. Not only do the dP traces in Fig. 4 indicate a much larger thermal expansion of the HOPG substrate, it also seems to be less stable mechanically after dipping into the C32/heptane solution. Possibly this is due to the intercalation of the solution between graphite microcrystallites. The intercalated heptane may diffuse

slowly throughout the HOPG substrate on the time scale of the experiment and eventually evaporate.

IV. DISCUSSION

There are several features of our ellipsometric and stray light data for C32 films adsorbed on SiO₂ that are compatible with the model proposed by Riegler and co-workers.^{4,7} We begin by reviewing the behavior of films having an average thickness greater than ~ 50 Å shown in Figs. 2(a)–2(c). First, we have already argued in the previous section that the abrupt transition to a high SLI upon heating which we observe in the temperature range $T_b < T < T_s$ is consistent with the melting of solid bulk particles to form liquid droplets of larger dimension. One expects the SLI to increase when scattering occurs from particles whose characteristic size has grown comparable to the wavelength λ of the incident light. Second, the abrupt drop to a low constant SLI for $T > T_s$ is consistent with interpreting T_s as the wetting temperature of C32 on the SiO₂ surface. Above T_s , a liquid C32 film forms of uniform thickness and with a surface roughness small compared to λ .

The complementary behavior of dP shown in Figs. 2(a)–2(c) where dP has a downward notch in the temperature range, $T_b < T < T_s$, is also consistent with the melting of solid bulk particles to form larger size liquid droplets. Since the ellipsometer light scatters isotropically from droplets of dimension comparable to its wavelength λ , such droplets atop a planar film (smooth on a length scale of λ) cannot contribute significantly to a rotation in the light polarization detected in the specularly reflected beam. Hence, if the number of molecules in the illuminated sample area remains constant but the number of such droplets increases, the film will appear thinner and the measured value of dP will decrease. We then expect dP to fall to a lower value for temperatures $T_b < T < T_s$ and remain constant as long as there is no change in the droplet size distribution and no desorption. If there are also solid particles of dimension comparable to λ below T_b , the step height in dP at T_b will depend on the ratio of the number of such particles to the number of droplets of this size above T_b . In Fig. 2(a), for example, the step is relatively large, suggesting that initially there are very few solid particles of dimension comparable to λ below T_b . However, in Figs. 2(b) and 2(c), the much smaller step in dP at T_b reflects both a larger average particle size when the sample is subsequently cooled below T_b .

When cooling the thicker films (average thickness $\geq \sim 50$ Å), we always observe an abrupt increase in the SLI below T_s . This feature is consistent with the dewetting transition from uniform liquid film to liquid droplets as discussed by Merkl *et al.*⁴ Our observation that the SLI remains constant as the sample is cooled below T_b [Figs. 2(a) and 2(b)] can be explained by the freezing of the droplets to form bulk crystallites of comparable size. We also note that for these thicker films, the SLI is lower at the beginning of the first heating-cooling cycle than at its end. This behavior of the SLI is consistent with our inference from dP in the heating portion of the cycle that after removing the samples from the C32/heptane solution there are either fewer large bulk par-

ticles present or that they have become larger by the time that they resolidify.

We next address the question of what features in our data might correspond to the solid monolayer phase proposed by Riegler and co-workers. From x-ray reflectivity measurements on several different alkane films,⁴ they inferred a monolayer of thickness on the order of the molecular length with a melting point at the wetting temperature T_s . Subsequently, their in-plane x-ray diffraction measurements⁷ showed Bragg peaks corresponding to monolayer d -spacings consistent with the long axis of the molecules oriented perpendicular to the SiO₂ surface. They also performed scanning force microscopy (SFM) measurements that revealed a fractal topology at submonolayer coverages.

To our knowledge, the anisotropy in the electric polarizability of the C32 molecules parallel and perpendicular to the chain axis has not been measured. A rough calculation suggests that the anisotropy is not large enough to allow determination of the molecular orientation in a VHRE experiment. Therefore, the identification of a monolayer phase characterized by a perpendicular molecular orientation requires a more indirect method.

We suggest that the signature in our VHRE experiments of the monolayer phase reported in Refs. 4 and 7 is the behavior that we have observed at coverages below that required for nucleation of solid bulk particles or bulk droplets, i.e., for average C32 film thicknesses in the range ~ 6 Å to ~ 50 Å in Figs. 2(b)–2(e) and Figs. 3(a)–3(c). For these film thicknesses, we observe a small upward step in dP at $T \sim 332$ K followed by the small downward substep near T_s . Although no anomaly was reported at $T \sim 332$ K by Riegler and co-workers,^{4,7} the downward substep near T_s occurs very close to the disordering temperature which they found for the solid monolayer phase. This feature thus provides the strongest link to the monolayer phase in their model.

To interpret the substep in dP at ~ 332 K in Figs. 2(b)–2(e) and Figs. 3(a)–3(c), we first consider what appears to be a related feature in the thicker films (average thickness ≥ 50 Å) which occurs at ~ 336 K [see Fig. 2(a)]. This temperature is very close to that at which there is a transition in bulk C32 to a plastic or rotator phase characterized by rotational disorder of the molecules about their long axis.¹⁸ In analogy to this phase transition in the bulk solid, we suggest that the substep in dP in the thinner films at ~ 332 K may correspond to a crystalline-to-plastic phase transition in the monolayer solid consisting of C32 molecules with their long axis oriented nearly perpendicular to the surface.^{4,7} For films of average thickness in the range ~ 6 Å to ~ 50 Å, we would expect the height of both substeps in dP to decrease as C32 molecules desorb from the substrate and the number of molecules in the fractal monolayer domains⁷ decreases. This appears to be the case for the thinner sample Si#3 in Figs. 3(a)–3(c).

We comment here that one would not expect a jump in dP corresponding to a decrease in the average film thickness of ~ 44 Å (the all-*trans* length of the C32 molecule) as a monolayer of perpendicularly oriented molecules is removed. Assuming a fractal topology for film thicknesses less than a molecular length as indicated by the SFM images,⁷ the

lateral averaging in the ellipsometric film thickness measurement should result in a continuous decrease in dP .

The monolayer phase adjacent to the SiO₂ surface proposed by Riegler and co-workers is unexpected in that, as inferred from their x ray measurements, the long-axis of the alkane molecules is oriented *normal* to the adsorbing surface. Previous experiments with alkane adsorption on graphite (0001),^{3,19} Cu(111),²⁰ Au(111),²⁰ Ag(111),²¹ and Pt(111)²² surfaces, using a wide variety of techniques, have always indicated a first layer in which the long molecular axis is *parallel* to the surface. In addition, molecular dynamics (MD) simulations of intermediate-length alkanes adsorbed on Au(001)²³ and graphite basal plane surfaces²⁴ show the molecules in the first layer to be parallel to the surface.

These previous experiments and MD simulations motivate us to speculate on the structure of the thinnest films in our ellipsometry experiments. The dP trace in Fig. 3(d) indicates that a film of average thickness ~ 6 Å remains even after the substeps in dP , the signature that we have assumed of a monolayer of perpendicularly oriented molecules, have disappeared. For this reason, we propose that there are actually more stable solid molecular layers immediately adjacent to the SiO₂ surface in which the long-axis of the C32 molecules is parallel to the interface. The monolayer phase proposed by Riegler and co-workers would then be adsorbed above these.

In support of this interpretation, recall that, for normal alkanes with carbon number $n < 30$, Merkl *et al.*⁴ inferred a monolayer thickness about 10% *greater* than the all-*trans* length of the molecule. This discrepancy of magnitude comparable to a molecular width can be explained by a layer of molecules oriented parallel to the surface underneath a monolayer of perpendicularly oriented molecules. It is difficult to explain otherwise, since any tilting of the molecules away from the surface normal would decrease the thickness of monolayer phase proposed in Refs. 4 and 7. Also, *gauche* defects known to be present in the molecules at room temperature^{23,24} would tend to reduce their end-to-end distance.

Our experiments thus lead us to consider a structure of the C32 adsorbed on SiO₂ similar to that found in molecular dynamics simulations by Xia *et al.* of liquid hexadecane (n -C₁₆H₃₄) films adsorbed on a Au(001) substrate at 350 K.²³ Their simulations indicate (see their Fig. 2) a more compact first layer in which the molecules are nearly parallel to the surface and in which the molecules have some degree of translational and orientational order. Above this layer and extending out to ~ 40 Å (the limit of their simulation) are molecules which tend to be more perpendicular to the surface and contain a larger number of *gauche* defects.

We suggest that a similar structure may occur at temperatures $T \lesssim 332$ K for C32 adsorbed on a SiO₂ surface as depicted in Fig. 5. Immediately adjacent to the SiO₂ interface are one to three layers of C32 (see below) in which the long molecular axis is oriented parallel to the interface. Above this “parallel” film would be the monolayer proposed in Refs. 4 and 7 in which the molecules are oriented more nearly perpendicular to the interface. Our model differs from the liquid structures found by Xia *et al.* in that both the “par-

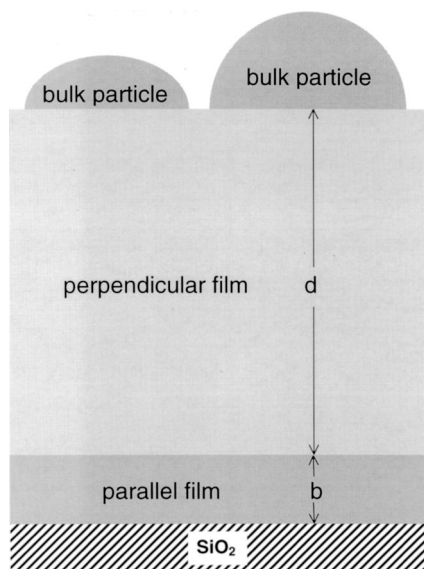


FIG. 5. Proposed model for the C32/SiO₂ interfacial region.

allel” and “perpendicular” films in Fig. 5 would constitute distinct *crystalline* phases. In particular, the upper phase would support a crystalline-to-plastic phase transition at ~ 332 K analogous to that which occurs in bulk C32 at ~ 336 K.¹⁸ The absence of substeps in dP up to ~ 380 K for films of average thickness less than ~ 6 Å indicates that a crystalline-to-plastic phase transition as well as a disordering transition at T_s either do not occur in the parallel film or that we lack the sensitivity to observe them. At higher coverages where we have inferred the nucleation of solid bulk particles, we observe a substep in dP at ~ 336 K and interpret it as resulting from the crystalline-to-plastic phase transition in these bulk particles.

To estimate the thickness “ b ” of the parallel film in Fig. 5, note that we have identified its presence by the disappearance of the substeps in dP occurring, e.g., between the third [Fig. 3(c)] and fourth [Fig. 3(d)] heating–cooling cycles of sample Si#3. Analysis of dP with a Drude model (see Sec. II) yields a film thickness of ~ 12 Å and ~ 6 Å at the beginning of the third and fourth cycles, respectively. Therefore, we infer an upper bound on b of ~ 12 Å which, assuming a molecular width of ~ 4.5 Å,²⁴ corresponds to a film in which the long-axis of the molecules is parallel to the interface having a thickness less than ~ 2.7 layers. The thickness “ d ” of the “perpendicular film” in Fig. 5 would be approximately equal to the all-*trans* length of the C32 molecule as in the model of Refs. 4 and 7.

Another estimate of the thickness b can be made by assuming that the perpendicular film in Fig. 5 is complete at the coverage at which we first observe the nucleation of bulk droplets in the temperature range $T_b < T < T_s$. This coverage occurs for sample Si#4 during its third heating–cooling cycle [Fig. 2(c)] in the interval between time t_1 when it passes through T_s on heating and t_2 when it returns to this temperature on cooling. Again, applying a Drude model, we infer the total film thickness, $d + b$, to be ~ 71 Å and ~ 52 Å at times t_1 and t_2 , respectively. Taking $d \sim 44$ Å,²⁴ the all-*trans* length of the C32 molecule, we obtain 8 Å $< b < 27$ Å. In this

way, we arrive at a weaker bound on the thickness of the parallel film of between two and six layers.

A question that arises at this point is why evidence of the parallel film was not observed in the in-plane synchrotron x-ray diffraction experiment.⁷ We can use the stronger bound of ~ 2.7 layers for the parallel film thickness to estimate the relative Bragg peak intensities of the parallel and perpendicular films. In Ref. 7, the structure inferred for the perpendicular monolayer gave an area per molecule of ~ 18.7 Å². This can be compared with a molecular area of 196 Å² found for a C32 monolayer adsorbed on the basal planes of graphite in which the long-axis of the molecules is parallel to the surface.²⁴ Assuming these areal densities and a parallel film with ~ 2.7 times as many layers as the perpendicular film, we conclude that the Bragg peaks of the parallel film should be about a factor of four times weaker than for the perpendicular film. Observation of the Bragg peaks could also be obscured by the roughness of the SiO₂/C32 interface resulting in a shorter coherence length in the parallel film compared to that obtained on graphite.²⁴ The perpendicular film might not be as sensitive to surface roughness since molecules oriented on end can adjust in height more easily.

The structural model in Fig. 5 suggests reevaluating the surface freezing mechanism that Merkl *et al.*⁴ have used to explain the structure at the alkane/SiO₂ interface. Since we infer a phase adjacent to the SiO₂ surface in which the molecules are oriented more nearly parallel to the surface, the structure no longer resembles that at the bulk alkane/air interface. Therefore, one would not necessarily expect the same theory²⁵ to be applicable to both interfaces.

V. CONCLUSION

Our ellipsometric measurements of the optical thickness of C32 films adsorbed on SiO₂-coated Si(100) substrates, which are conducted in air, have demonstrated a resolution and long-term stability comparable to that previously obtained with rare gases adsorbed on HOPG substrates in ultrahigh vacuum. They reveal a rich structure in the temperature dependence of the polarization angle and stray light intensity previously unobserved with alkane films.

Our results are consistent with the three different wetting topologies proposed by Merkl *et al.*⁴ However, they differ from their model in an essential way by requiring between one and three molecular layers adjacent to the SiO₂ surface in which the long-axis of the C32 molecules is parallel to the interface. Such a parallel film phase is similar to those inferred in all previous experiments on normal alkanes adsorbed on solid substrates. Moreover, it suggests a different structural mechanism for the alkane/SiO₂ interface than has been proposed for the bulk alkane/air interface.

Our measurements on thicker films do not offer direct evidence of a monolayer containing molecules with their long axis oriented more nearly perpendicular to the interface. However, we observe a substep in the temperature dependence of the polarization angle which is not present in films of average thickness less than ~ 6 Å and which agrees with the melting point attributed to the monolayer phase by Merkl *et al.* In addition, we observe a second substep in dP at ~ 332 K which appears to be associated with such a phase.

We have suggested that it may result from a crystalline-to-plastic transition in the monolayer phase that Merkl *et al.* have proposed. This conclusion was based on a similar sub-step that we observed at ~ 336 K, for coverages above that required for bulk nucleation, which matched the known crystalline-to-plastic transition temperature of bulk C32.

Finally, for high alkane coverages, we have presented a model of the alkane/SiO₂ interfacial structure (see Fig. 5) that is consistent with our polarization angle and stray light intensity measurements as well as the x-ray specular reflectivity measurements of Riegler and co-workers.^{4,7} Below ~ 332 K, it consists of solid layers immediately adjacent to the SiO₂ surface in which the long-axis of the molecules is parallel to the interface and above which is a layer of perpendicularly oriented molecules. Atop these film phases, incomplete wetting of the C32 results in the coexistence of solid bulk particles.

Further study is necessary to test the model in Fig. 5. We are conducting molecular dynamics simulations similar to those of Xia *et al.*²³ but at temperatures low enough for the alkane adsorbate to solidify. Also, the model in Fig. 5 predicts a total C32 film thickness that exceeds the all-*trans* length of the C32 molecule by about 6–12 Å. X-ray specular reflectivity experiments on the same samples used for ellipsometric measurements are in progress to test this prediction.

ACKNOWLEDGMENTS

The authors thank K. W. Herwig and H. Mo for helpful discussions and S. Alegria for assistance in the sample preparation. They are indebted to K. Knorr for many discussions and a critical reading of the manuscript. This work was supported by the Chilean government under CONICYT Grant No. 018/AT/005NSF and FONDECYT Grant No. 1980586 and by the U.S. National Science Foundation under Grant Nos. INT-9605227, DMR-9802476, and DMR-0109057.

- ¹G. B. Hess, in *Phase Transitions in Surface Films 2*, edited by H. Taub, G. Torzo, H. J. Lauter, and S. C. Fain, Jr., NATO Advanced Study Institute, Ser. B, Vol. 267 (Plenum, New York, 1991), p. 357.
- ²U. G. Volkman and K. Knorr, *Surf. Sci.* **221**, 379 (1989).
- ³K. W. Herwig, B. Matthies, and H. Taub, *Phys. Rev. Lett.* **75**, 3154 (1995).
- ⁴C. Merkl, T. Pfohl, and H. Riegler, *Phys. Rev. Lett.* **79**, 4625 (1997).
- ⁵T. Pfohl, D. Beaglehole, and H. Riegler, *Chem. Phys. Lett.* **260**, 82 (1996).
- ⁶A. Asmussen and H. Riegler, *J. Chem. Phys.* **104**, 8159 (1996).
- ⁷A. Holzwarth, S. Leporatti, and H. Riegler, *Europhys. Lett.* **52**, 653 (2000).
- ⁸X. Z. Wu, E. B. Sirota, S. K. Sinha, B. M. Ocko, and M. Deutsch, *Phys. Rev. Lett.* **70**, 958 (1993); X. Z. Wu, B. M. Ocko, E. B. Sirota, S. K. Sinha, M. Deutsch, B. H. Cao, and M. W. Kim, *Science* **261**, 1018 (1993).
- ⁹U. G. Volkman, H. Mannebach, and K. Knorr, *Langmuir* **14**, 4904 (1998).
- ¹⁰P. Drude, *Ann. Phys. Chem.* **39**, 481 (1890).
- ¹¹R. M. A. Azzam and N. M. Bashara, *Ellipsometry and Polarized Light* (North-Holland, Amsterdam, 1977).
- ¹²D. V. Sivukhin, *Zh. Eksp. Teor. Fiz.* **18**, 976 (1948); **21**, 367 (1951); *Sov. Phys. JETP* **3**, 269 (1956).
- ¹³M. J. Dignam and J. Fedyk, *J. Phys. (France)* **38**, C5 (1977).
- ¹⁴*CRC Handbook of Data on Organic Compounds*, edited by Robert C. Weast and Melvin J. Astle (CRC, Boca Raton, 1985), Vol. 1, p. 586.
- ¹⁵*Handbook of Chemistry and Physics*, 79th ed., edited by David R. Lide (CRC, Boca Raton, 1998–1999).
- ¹⁶The Si(100) wafers were made by Aurel GmbH, Malteserstr. 443 C, D-86899 Landsberg, Germany.
- ¹⁷H. Mo, H. Taub, U. G. Volkman, M. Pino, S. N. Ehrlich, D. S. Robinson, F. Y. Hansen, E. Lu, and P. Miceli (unpublished).
- ¹⁸D. M. Small, *The Physical Chemistry of Lipids: From Alkanes to Phospholipids* (Plenum, New York, 1986), p. 195.
- ¹⁹H. Taub, in *The Time Domain in Surface and Structural Dynamics*, NATO Advanced Study Institute, Series C: Mathematical and Physical Sciences, edited by G. J. Long and F. Grandjean, Vol. 228 (Kluwer, Dordrecht, 1988), p. 467.
- ²⁰J. Weckesser, D. Fuhrmann, K. Weiss, Ch. Wöll, and N. V. Richardson, *Surf. Rev. Lett.* **4**, 209 (1997).
- ²¹Z. Wu, S. N. Ehrlich, B. Matthies, K. W. Herwig, Pengcheng Dai, U. G. Volkman, F. Y. Hansen, and H. Taub, *Chem. Phys. Lett.* **348**, 168 (2001).
- ²²D. Fuhrmann, A. P. Graham, L. Criswell, H. Mo, B. Matthies, K. W. Herwig, and H. Taub, *Surf. Sci.* **482–485**, 77 (2001).
- ²³T. K. Xia, Jian Ouyang, M. W. Ribarsky, and U. Landman, *Phys. Rev. Lett.* **69**, 1967 (1992).
- ²⁴F. Y. Hansen, K. W. Herwig, B. Matthies, and H. Taub, *Phys. Rev. Lett.* **83**, 2362 (1999).
- ²⁵A. V. Tkachenko and Y. Rabin, *Phys. Rev. Lett.* **76**, 2527 (1996).